Regular Article

PHYSICAL CHEMISTRY RESEARCH
Published by the
Iranian Chemical Society
www.physchemres.org
info@physchemres.org

Phys. Chem. Res., Vol. 12, No. 1, 121-133, March 2024

817M40T Mild Steel Corrosion Remediation in 0.5 M Hydrochloric Acidic Environment Using Alkaloid and Flavonoid Extracts of Salvia Officinalis

Benedict Ushaka Ugi[a,*] and Fredrick Bekong Ugi[b]

[a]*Department of Pure & Industrial Chemistry, Faculty of Physical Sciences, University of Calabar, P. M. B. 1115, Nigeria*

[b]*Chemical/Petrochemical Engineering Department, Rivers State University, Port Harcourt-Nigeria*

(Received 7 September 2022, Accepted 29 April 2023)

Alkaloid and Flavonoid extracts of *Salvia Officinalis* Leaves (AESOL and FESOL) as eco-friendly corrosion inhibitors of 817M40T Mild Steel in 0.5 M Hydrochloric acid (HCl) concentrated environment were carried out. Weight loss, thermometric, electrochemical impedance spectroscopy, and potentiodynamic polarization techniques were employed. The corrosion rate values of the alkaloid and flavonoid were seen to be in decrease from 1.6-0.01 and 1.6-0.1 while the inhibition efficiency values were observed to increase from 79.7%-99.3% and 75.1%-93.8% for alkaloid and flavonoid fractions respectively at concentrations of 150-1000 ppm which defined the inhibitors a good inhibitor. A slight effect of temperature on the inhibition process was observed from the thermometric result as temperature was increased owing to strong agitation of heat. Electrochemical data showed that charge transfer resistance and inhibition efficiency were increasing while double-layer capacitance and corrosion current density values were decreasing with concentration. A mixed-type inhibition was recorded while the adsorption process proved that the inhibitors were a monolayer type and physically adsorbed. Thermodynamic data revealed an inhibitor that is stabled, spontaneous, associative, and endothermic in reaction.

Keywords: Mild steel, Flavonoids, Inhibitor, Corrosion, Adsorption, Alkaloid

INTRODUCTION

Corrosion constitute enormous lose amongst the other factors that are a disadvantage to the sector. Corrosion in itself is an electrochemical process taking part on material at major corrosion active sites which constitutes more of the anodic areas and some parts of the cathodic areas [1-2]. It most likely occurs under conditions of moisture and air, the presence of electrolyte and a possibility of electron migration from the anodic electrode or sites due to dissolution giving rise to oxidation [1-3]. The struggle to combat corrosion effects on materials especially metals has come a long way comprising the use of different protective measures, especially environmental modifications, metal selection, and surface conditions, and now eco-friendly inhibitors from expired drugs not just for the sake of corrosion retardation but recycling as well [1-5]. Organic corrosion inhibitors have always been associated with a variety of organic compounds with mainly heteroatoms such as Phosphorus (P), Nitrogen (N), Sulphur (S), and Oxygen (O) [3,4-10]. These atoms coordinate with the corroding metal ions through their electrons, hence forming protective films which reduce the corrosion action. Organic corrosion inhibitors are based on the adsorption on the surface to form protective film which displaces water from the metal surface and protects it against deterioration [5,11]. This process is not either purely physical or purely chemical adsorption. A lot of sectors especially the chemical, petroleum, marine, mechanical, *etc*. make use of acids especially hydrochloric and sulphuric acids almost routinely in different operations sanding from acid pickling, cleansing, scale removal from pipes, acidization which involves pumping dilute acids into drilled well or geological formation that is capable of producing oil and/or gas [2-4,11-14]. Corrosion in the oil and gas sector most importantly

*Corresponding author. E-mail: ugibenedict@gmail.com

affects as much as flow lines, gathering and feeder lines, crude trunk pipelines, petroleum products trunk pipelines. S275JR mild steel is one of the most commonly used grades in general construction. It is an un-alloyed, hot-rolled, low-carbon mild steel [3,10]. 817M40T is available in a wide choice of profiles and presentations. It is easy to cut, weld, machine, and drill which makes it the perfect choice to use for frames, vehicles, joist supports, lintels, shelves, brackets, construction, and maintenance projects. This research aimed at proffering a possible corrosion inhibition pathway that will have less or no consequence on the eco-system but reduce or eliminate where possible the effects of corrosion on 817M40T Mild Steel deployed for use at various metallurgical sectors of the economy through the use of *Salvia officinalis* herbal plant phytochemicals (alkaloids and flavonoids) Fig. 1.

MATERIALS AND METHODS

817M40T Mild Steel Resizing and Dressing

The sheet of 817M40T Mild Steel deployed for the research has the following chemical composition: Zn (0.005%) and Fe (99.34%), C (0.19%), Si (0.20%), Na (0.64%), S (0.05%), P (0.06), Ni (0.09%), Cr (0.08%), Mo (0.02%) and Cu (0.21%) respectively and were obtained commercially from System Metals Nig. Ltd. Calabar, Nigeria. The sheets were mechanically press-cut into 3.00 × 0.05 × 3.00 cm coupons. These were polished with different grades of emery paper ranging from 200-1200 grades and rinse in distilled water, degreased in absolute ethanol, dried in acetone, and stored in a moisture-free desiccator prior to use. The aggressive acidic solution of 0.5 M HCl was prepared by dilution of analytical grade HCl with distilled water at right proportion. All experiments were carried out in unstirred solutions and all weighing were done with a digital analytical balance.

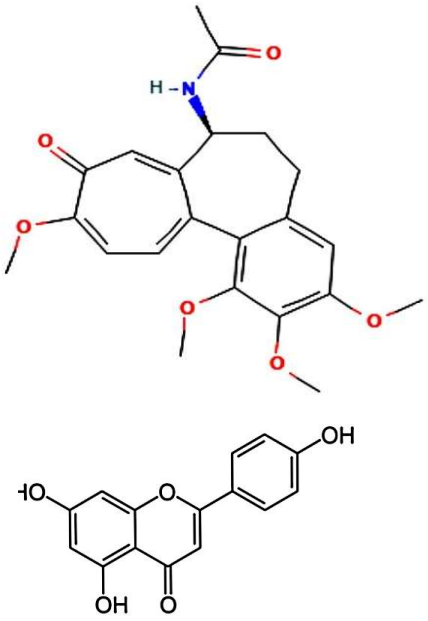

Fig. 1. Structures of main alkaloids (colchicine) and flavonoid (apigenin) of *Salvia officinalis. Source: Pubchem: http:/pubchem.ncbi.nlm.nih.gov.*

Preparation of Salvia Officinalis Leaves

The fresh leaves of *Salvia officinalis* herbal plant collected from a reserved forest around the Central zone of Cross River State, Nigeria were washed, aired dried for 24 h, and further dried in a laboratory Oven at a minimal temperature to avoid loss of major organic components of the plant for 48 h. The dried leaves collected from the Oven were then ground into powder form to obtain a fine particle structure for easy extraction. The powdered sample was extracted continually with absolute ethanol in a Soxhlet Extractor for over 24 h. The extract obtained was later heated on a water bath at a regulated temperature of 60 °C until most of the ethanol evaporated. 15 g of the crude ethanol extract was diluted with 1litre volume of the 0.5 M HCl solution and then kept for approximately 24 h.

Alkaloid and Flavonoid Extraction and Inhibitor Preparation

Dilute hydrochloric acid (35.5% w/w) and Ammonia solution was used. The HCl employed during the experiment was less than 1 M, but not weaker than 0.1 M (pH 0-1). 50 g of the ethanol extract was partitioned between 100 ml of chloroform and 100 ml of 0.1 M HCl solution using a separating funnel. The HCl solution in the float fraction from the separating funnel was carefully basified with Ammonia solution and this was taken well above pH 7. A white cloud formed in the solution was noticed indicative of alkaloids presence. Chloroform was immediately added to the basic solution in the separating funnel and two clear layers were

formed with the lower one (organic) containing the alkaloids. The chloroform layer was eventually separated from the mixture and put aside, the chloroform distilled off, and a small quantity of moderately pure alkaloids was obtained. 5 g of the alkaloid extract was soaked in 0.5 l of 0.5 M HCl solution and kept for 24 h. The solutions obtained were filtered and stored. Meanwhile, the flavonoid extracts, 10 g of powdered sample of the leaf was weighed and digested in 100 ml methanol for 5 h. The digested solution was then filtered and concentrated over a water bath at 60 °C to remove almost all the methanol solution.

From the stock solution (5 g l^{-1}), inhibition test solutions were prepared to obtain 150 ppm, 250 ppm, 350 ppm, 500 ppm, and 1000 ppm for mass loss and thermometric measurements respectively.

Gravimetric Experimentation

The gravimetric experiment was carried out employing different concentrations of the inhibitors. 100 ml beakers were used to host the inhibitor solutions while suspended resized metals were weighed and immersed in the inhibited solution. Each exercise was allowed for 60 min after which the metals were taken out, washed through running water using a bristle brush, degreased using ethanol, rinsed in acetone, and air dried then weighed again. The process for each inhibitor was carried out for 360 min. The measurements were repeated twice and the average of the values were obtained. Data generated from the weight loss experiment were used to calculate the corrosion rate (Ƈ) of the metal, surface coverage (θ), and inhibition efficiency (% IЄ) of the inhibitor using Eqs. (2) and (3).

$$\theta = \frac{Ƀr_0 - Ƀr_i}{Ƀr_0} \quad (1)$$

$$IЄ\,\% = \frac{Ƀr_0 - Ƀr_i}{Ƀr_0} \times 100 \quad (2)$$

where $Ƀr_0$ and $Ƀr_i$ are the loss in weight for the 0.5 M HCl and inhibited solutions respectively, and IЄ% is the inhibition efficiency.

Thermometric Experimentation

250 ml beakers were used to host the inhibitor solutions while suspended resized metals were immersed in the inhibited solution after an initial weight of metals was taken. This experiment was conducted at regulated temperatures of 303, 313, and 333 K using a water bath. Each exercise was allowed for 60 minutes after which the metals were taken out, washed through running water using a bristle brush, degreased using ethanol, rinsed in acetone, and air dried then weighed again. The process for each inhibitor was carried out for 360 min. Data generated from the experimentation were used to obtain the corrosion rate (Ƈ) of the metal, surface coverage (JЬ), and Inhibition efficiency (% IЄ) of the inhibitor following Eqs. (3) and (4).

$$JЬ = \frac{ƈ_0 - ƈ_i}{ƈ_0} \quad (3)$$

$$IЄ\,\% = \frac{ƈ_0 - ƈ_i}{ƈ_0} \times 100 \quad (4)$$

where $ƈ_0$ and $ƈ_i$ are the loss in weight for the blank and inhibited solutions respectively, and IЄ% is the inhibition efficiency of the inhibitors.

Electrochemical Impedance Spectroscopy (EIS) Technique

Electrochemical impedance spectroscopy test was carried out at 303 K in a three-electrode cell using Gamry Reference 600 potentiostat/Galvanostat inclusive of a Gamry framework EIS300 system. Echem Analyst software was used for analyzing and fitting data. The frequency range was 100 kHz-0.01 Hz and an AC signal amplitude of 10 mV was used. Platinum electrode was used as counter electrode and saturated calomel electrode (SCE) was used as the reference electrode while the working electrode was 1 cm^2 by dimension. Measurements were performed in aerated solution after 25 min of immersion in the test solution at ambient temperature in order to attain a steady-state open-circuit potential (OCP). The Nyquist plots derived in the absence and presence of alkaloid and flavonoid inhibitors were fitted in the suitable equivalent circuit in order to obtain some useful kinetic parameters, including the charge transfer resistance ($ß_{cti}$). Inhibition efficiency, ß% was calculated from charge transfer resistance $ß_{cti}$ of inhibitors, according to Eq. (5).

$$IЄ\% = \frac{ß_{cti} - ß_{cto}}{ß_{cti}} \times 100 \quad (5)$$

where δ_{ct} and δ_{cti} represents the charge transfer resistance without and with AESOL and FESOL, respectively.

Potentiodynamic Polarization (PDP) Technique

PDP tests were performed at 303 K using the same instrument as EIS and the same data analyzer software. The PDP curves were measured at a scan rate of 0.5 mV s^{-1} from -0.25 to + 0.25 V *vs.* SCE. Anodic and cathodic Tafel curves for the dissolution of metals with and without inhibitors were recorded. Linear segments of the anodic and cathodic curves were extrapolated from the plots which gave useful thermodynamic parameters. The corrosion current density (I_{corr}) was used to calculate inhibition efficiency, Ⱶ% of inhibitors, according to Eq. (6)

$$Ⱶ\% = \left[1 - \frac{I^0_{corr}}{I^i_{corr}}\right] \times 100 \quad (6)$$

where $I°_{corr}$ and I_{corr} represent corrosion and current density obtained without and with AESOL and FESOL, respectively.

Scanning Electron Microscopy (SEM)

Scanning electron microscope, model number JSM-5600 LV, Tokyo, Japan was used to produce micrographs of the metal coupon without (0.5 M HCl solution) and with inhibition. Selected coupons were retrieved from the test solution after 6 h of immersion. Each sample was mounted on a metal stub and sputtered with gold. Scanned micrographs were taken at an accelerating voltage of 1.5 and 12.00 kV.

RESULT AND DISCUSSION

Gravimetric Results

The efficacy of both alkaloids and flavonoid fractions as inhibitors was examined through weight loss procedures. The data obtained through the plot of weight loss of metal in mg against the time of immersion of the metal in both inhibitors has been analyzed and presented in Table 1. The strength of the inhibitors in combating the negative effect of the hydrochloric acid on 817M40T-Typed Mild Steel is recorded in the corrosion rate values which were seen to be in the decrease from 1.6-0.01 and 1.6-0.1 for alkaloid and flavonoid fractions respectively at increasing concentrations of 150 ppm-1000 ppm. This appreciable characteristic of the inhibitor could be attributed to its strong adsorption on the metal active sites capable of initiating corrosion [10,15]. This was confirmed from the strong inhibition efficiency values recorded between 79.7%-99.3% and 75.1%-93.8% for alkaloid and flavonoid fractions respectively at increasing concentrations of 150 ppm-1000 ppm. This again proved that both inhibitors were able to increase the inhibitor surface coverage and reduce to its barest minimum the anodic dissolution and cathodic hydrogen evolution tendencies hence mitigated the corrosion process [5,9,17].

Thermometric Analysis Result

In response to the effect of temperature on the viability of alkaloid and flavonoid fractions as inhibitors, gasometric results were obtained for the inhibitor as presented in

Table 1. Weight Loss Values for Inhibition of 817M40T-Mild Steel Without and with AESOL and FESOL in 0.5 M HCl Acid

	AESOL			FESOL		
Systems	CR ($mg/cm^2/min$)	Surface coverage (Θ)	Ⱶ (%)	CR ($mg/cm^2/min$)	Surface coverage (Θ)	Ⱶ (%)
0.5 M HCl	1.609	-	-	1.609	-	-
150 ppm	0.327	0.797	79.7	0.400	0.751	75.1
250 ppm	0.219	0.864	86.4	0.374	0.768	76.8
350 ppm	0.165	0.897	89.7	0.326	0.797	79.7
500 ppm	0.100	0.938	93.8	0.192	0.881	88.1
1000 ppm	0.012	0.993	99.3	0.100	0.938	93.8

Tables 2 and 3. The strength of the inhibitors is recorded in the corrosion inhibition efficiency values which were seen to be in increase from 60.2-99.5% and 19.6-62.9 for alkaloid and flavonoid fractions respectively at increasing concentrations of 150 ppm-1000 ppm. It was also observed that the result showed a physical nature of adsorption following the higher inhibition efficiency of both inhibitors at the ambient temperature of 303 K [10,12-13,18]. The decreased inhibition efficiency with temperature and correspondent increased corrosion rate as observed with the mild steel in Tables 2 and 3 does not only indicate a physical adsorption process but explains the possibility of losing the weakly bounded inhibitor molecules due to the temperature agitation effect [12-15,19]. The desorption process shows that the inhibitor still inhibits the 817M40T-Typed Mild Steel surface at higher temperatures but better at lower temperatures and this can again be attributed to the stronger adsorption of inhibitor molecules on the mild steel surface where the corrosion reaction rate is minimal [2,8,16].

Potentiodynamic Polarization Results

Calculated values of Potentiodynamic polarization parameters were obtained from Figs. 2a-b. The inhibition efficiency for the tested inhibitors was in good agreement with those calculated from both weight loss and thermometric experiments. The inhibition efficiency of the inhibitors rose from 65.8-94.2% for alkaloid fraction and 63.9-87.2% for flavonoid fraction between concentrations of 150 ppm and 1000 ppm, respectively. The values for the I_{corr} and E_{corr} were obtained from the extrapolation of the anodic and cathodic Tafel plots to the value of E_{corr} by the software provided with the equipment From Table 4, the results also

Table 2. Thermometric Analysis Values for Inhibition of 817M40T-Mild Steel without and with AESOL in 0.5 M HCl Acid

	CR (mg/cm^2/h)			θ			%IE		
Conc. (ppm)	303 K	313 K	333 K	303 K	313 K	333 K	303 K	313 K	333 K
0.5 M HCl	5.111	8.320	13.276	-	-	-	-	-	-
150 ppm	2.032	4.123	6.902	0.602	0.504	0.480	60.2	50.4	48.0
250 ppm	1.261	3.197	5.261	0.753	0.616	0.604	75.3	61.6	60.4
350 ppm	0.944	2.999	5.920	0.815	0.640	0.554	81.5	64.0	55.4
500 ppm	0.419	2.010	3.754	0.918	0.758	0.717	91.8	75.8	71.7
1000 ppm	0.028	1.538	2.900	0.995	0.815	0.782	99.5	81.5	78.2

Table 3. Thermometric Analysis Values for Inhibition of 817M40T-Mild Steel without and with FESOL in 0.5 M HCl Acid

	CR (mg/cm^2/h)			θ			%IE		
Conc. (ppm)	303 K	313 K	333 K	303 K	313 K	333 K	303 K	313 K	333 K
0.5 M HCl	5.111	8.320	13.276	-	-	-	-	-	-
150 ppm	4.109	6.902	11.763	0.196	0.170	0.114	19.6	17.0	11.4
250 ppm	3.107	5.749	9.985	0.392	0.309	0.248	39.2	30.9	24.8
350 ppm	3.016	4.713	9.793	0.410	0.434	0.262	41.0	43.4	26.2
500 ppm	1.894	3.278	6.195	0.629	0.606	0.533	62.9	60.6	53.3
1000 ppm	0.286	1.542	3.847	0.944	0.815	0.710	94.4	81.5	71.0

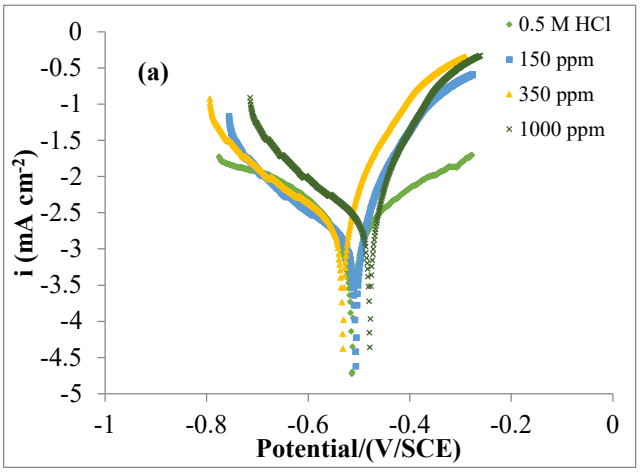

Fig. 2. Tafel plots for the corrosion inhibition of 817M40T-Mild Steel without and with (a) AESOL and (b) FESOL in 0.5 M HCl acid.

show that in the presence of both alkaloids and flavonoid inhibitors, i_{corr} values decreased steadily. This value suggests that AESOL and FESOL act as an efficient corrosion inhibitor against 817M40T-Typed Mild Steel corrosion in 0.5 M HCl acidic solution [15,19]. Again, as arrived at in Figs. 2a-b and Table 4 the addition of AESOL and FESOL molecules shifted the corrosion potential (E_{corr}) slightly to a more positive direction and also shows changes in both the cathodic and anodic polarization branches. These results indicate that the inhibitors acted as a mixed-type inhibitor [9, 12,20-21].

Electrochemical Impedance Results

The electrochemical parameters ranging from charge transfer resistance, double layer capacitance, and solution inhibition efficiency for both effects of alkaloids and flavonoids fractions of S. *officinalis* L are presented in Table 5 and the Nyquist plots and electrochemical circuit for the EIS are presented in Figs. 3-4. The model for Fig. 4 consists of an inductor, a capacitor, and two resistors to regulate the amount of current running through the circuit. However, a close study of Figs. 3a-b clearly reveals only one capacitive loop in the Nyquist plots, which could be attributed to a single charge transfer [10-13,19-23]. The size of these loops for both isolates increases with increasing concentration signifying perfect adsorption of the isolates on the 817M40T-Typed Mild Steel in 0.5 M HCl acid surface,

Table 4. Potentiodynamic Polarization Values for Inhibition of 817M40T-Mild Steel without and with AESOL and FESOL in 0.5 M HCl Acid

	Conc.	I_{corr} (mA cm^{-2})	E_{corr} (mV)	βc (mV dec^{-1})	βa (mV dec^{-1})	IEi (%)
	0.5 M HCl	0.910	-411.80	158	110	-
Alkaloids	150 ppm	0.311	-405.40	123	99	65.8
fraction of S.	250 ppm	0.197	-415.12	118	82	78.4
officinalis L	350 ppm	0.105	-400.04	112	61	88.5
	500 ppm	0.094	-389.11	83	56	89.7
	1000 ppm	0.053	-376.38	55	47	94.2
Flavonoids	150 ppm	0.328	-419.31	146	110	63.9
fraction of S.	250 ppm	0.301	-406.74	129	93	66.9
officinalis L	350 ppm	0.296	-385.06	121	88	67.5
	500 ppm	0.172	-329.05	100	81	81.1
	1000 ppm	0.117	-294.92	81	70	87.2

and the area exposed to the corrosive solution was reduced [4,11,18]. Increased values of charge transfer resistance in inhibited solution against those of the free acid was observed (Table 5). This observation usually follows the stronger adsorption of inhibited molecule on the metal surface hence deterring the transfer of charges between corrosion media and the metal active sites prone to corrosion giving rise to reduced anodic dissolution [1,3,24]. Charging and discharge of the capacitor is dependent on the ion adsorption mechanism of the electric double layer. Once ions are drawn over the electric double layer when voltage is applied, the capacitor is charged and the corrosion process begins [16,22, 25]. From Table 5, an observed decrease in values of double-layer capacitance was recorded implying that there was a move away of the charged ions from the metal layer as the inhibitor concentration was increased. This is an indication of perfect adsorption of inhibitor molecules over the capacitor (tested metal) [22,25-26]. The efficiency of these phytochemical compounds (alkaloids and flavonoids) has been further confirmed through the inhibition efficiency as calculated in Table 5.

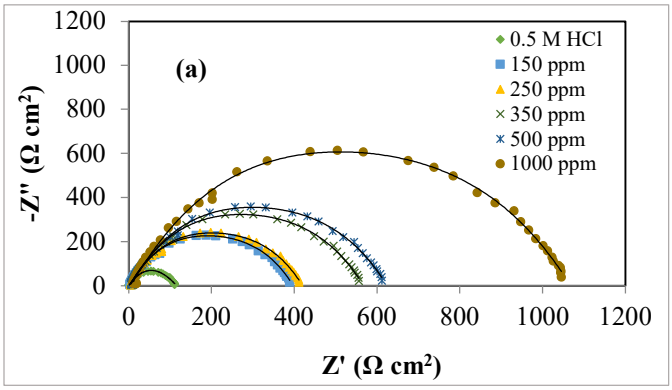

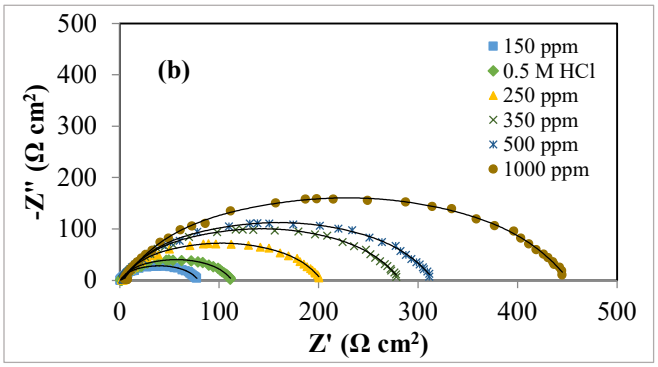

Fig. 3. Nyquist graphs depicting the inhibition of 817M40T-Mild Steel without and with (a) AESOL and (b) FESOL in 0.5 M HCl acid.

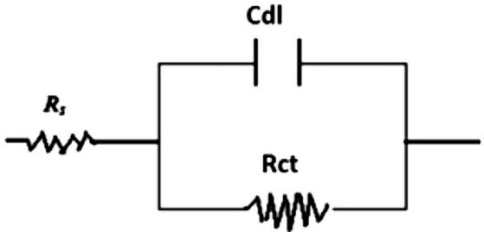

Fig. 4. Electrochemical equivalent circuit diagram for the inhibition of 817M40T-Mild Steel in 0.5 M HCl acid.

Table 5. Nyquist Values for Inhibition of 817M40T-Mild Steel without and with AESOL and FESOL in 0.5 M HCl Acid

	Conc.	Rct (Ω cm^{-2})	C_{dl} (μF cm^{-2})	IER (%)
	Blank (0.5 M HCl)	79	6.3×10^{-4}	-
Alkaloids fraction of S. officinalis L.	150 ppm	317	1.5×10^{-4}	75.1
	250 ppm	330	0.3×10^{-4}	76.0
	350 ppm	469	4.8×10^{-5}	83.2
	500 ppm	529	3.7×10^{-5}	85.0
	1000 ppm	1098	2.6×10^{-5}	92.8
Flavonoids fraction of S. officinalis L	150 ppm	94	4.1×10^{-4}	16.0
	250 ppm	122	2.6×10^{-4}	35.3
	350 ppm	209	0.6×10^{-4}	62.2
	500 ppm	236	0.5×10^{-4}	66.5
	1000 ppm	469	0.3×10^{-4}	83.2

Thermodynamic Approach

Table 6 values were drawn from the plots of ln CR against 1/T as shown in Figs. 5a-b using Eq. (7),

$$Ϛ = A \exp(\frac{-Ea}{RT}) \quad (7)$$

where Ϛ is the corrosion rate, A is the collision constant, R is the universal gas constant, T is the temperature (in kelvin), and E_a is the amount of energy required to ensure that a reaction happens (activation energy).

By taking the log of Eq. (7), Eq. (8) was obtained.

$$ln\, ς = ln\, A - \frac{Ea}{RT} \quad (8)$$

Increasing values for E_a in inhibited solution for both alkaloid and flavonoid extracts were recorded as against their blank value meaning that there was a reduction in the frequency of successful molecular collision, hence slowing the corrosion reaction [3,9,19-23]. It also confirms a physical adsorption process as its values were within the threshold of 20 kJ mol^{-1} [1,24-26]. The result from Table 6 showed increase values of "A" with increasing concentration of inhibitors which implies an increase in effective molecular collision of the inhibitors on the 817M40T-Mild Steel in 0.5 M HCl acid [16, 21,27-30].

Thermodynamic parameters were determined using the linear Eyring equation given in Eq. (9) [19,22,31-33]

.

$$ln\frac{ς}{T} = -\frac{ΔH}{R}\frac{1}{T} + ln\frac{kB}{h} + \frac{ΔS}{R} \quad (9)$$

where Ϛ is the corrosion rate, T is the absolute temperature,

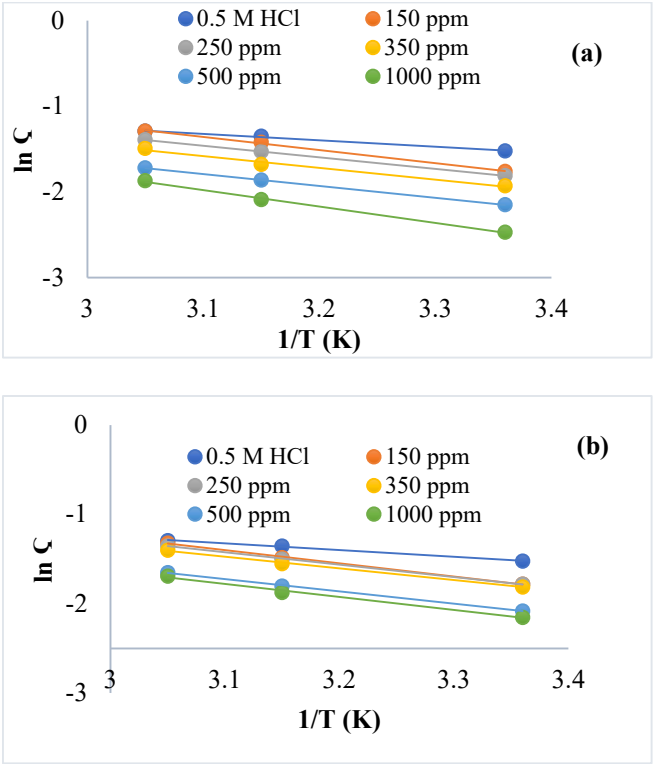

Fig. 5. Arrhenius plots for inhibition of 817M40T-Mild Steel without and with (a) AESOL and (b) FESOL in 0.5 M HCl acid.

$ΔH$ is the enthalpy of adsorption, $ΔS$ is the entropy of adsorption, kB is the Boltzmann constant, h is the plank constant and R, the universal gas constant. The values for $ΔH$ and $ΔS$ can be determined from kinetic data obtained from a $ln\frac{ς}{T}$ *vs.* $\frac{1}{T}$ plot. The Equation is a straight line with a negative slope, $-\frac{ΔH}{R}$, and a y-intercept, $ln\frac{kB}{h} + \frac{ΔS}{R}$.

Table 6. Thermodynamic Values for Inhibition of 817M40T-Mild Steel without and with AESOL and FESOL in 0.5 M HCl Acid

	TEMSS			AEMSS		
Conc.	E_a	$ΔH_{ads}$ (kJ mol^{-1})	$ΔS_{ads}$ (kJ mol^{-1})	E_a	$ΔH_{ads}$ (kJ mol^{-1})	$ΔS_{ads}$ (kJ mol^{-1})
0.5 M HCl	5.8	-7.3	-73.0	5.8	-7.3	-73.0
150 ppm	10.8	-14.5	-145.6	11.9	-14.8	-148.9
250 ppm	11.5	-15.0	-150.9	12.0	-16.3	-163.9
350 ppm	11.6	-15.6	-156.5	12.2	-16/6	-166.1
500 ppm	12.4	-17.9	-169.4	12.6	-17.1	-171.3

From Eq. (9), the plots in Figs. 6a-b were obtained and the data obtained are displayed in Table 6. Entropy values were negative for both inhibitors, an indication of a lower amount of disorder and increase adsorption of the inhibitor molecules [19-21,32]. Enthalpy values within the threshold of 80 kJ mol^{-1} explain physical adsorption and this was noticed for both inhibitors [25]. Also, positive values of enthalpy depict endothermic reaction meaning heat was gained by the system in the process of reaction, hence breaking up the intermolecular forces leading to a slower corrosion reaction rate [10-11,33].

Adsorption Isotherm Elucidation

Langmuir adsorption isotherm was used to verify the nature of the mechanism of action presented by both alkaloid and flavonoid inhibitors. The Langmuir plots of C/Θ against concentration (ppm) was adopted (Fig. 6) drawn from Eq. (10).

$$\frac{C}{\theta} = \frac{1}{k} + C \qquad (10)$$

Table 7 shows the data obtained from the plots in Fig. 7. It was observed that the equilibrium constant values (k) in inhibited solution were decreased with increased temperature. This phenomenon is always suggestive of physical adsorption mechanism as it is already confirmed from the temperature-dependent result (thermometric analysis) [29-35]. This result also indicates that there was room for a speedy migration of the molecules in solution enabling stronger bond formation between the inhibitor and the metal [29,31,36]. The values of the correlation coefficient were approximately unity, this implies that the data fitted well to the adsorption isotherm hence obeying the Langmuir assumption of monolayer adsorption [3,16,32]. The adsorption-free energy values were observed to be negative and less than -20 kJ mol^{-1} which defined the phenomenon of physical adsorption, spontaneity to the forward direction and increased inhibitor stability [30,34-40].

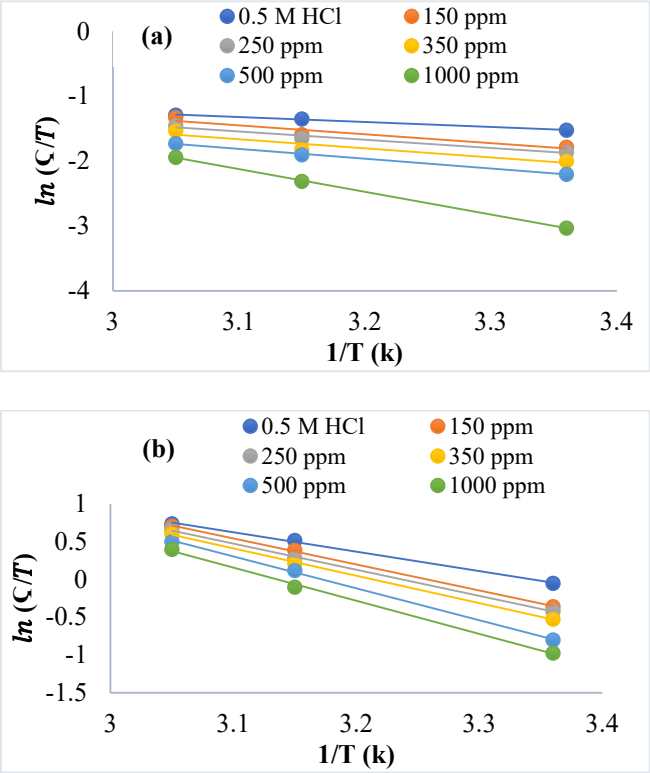

Fig. 6. Transition state plots for inhibition of 817M40T-Mild Steel without and with (a) AESOL and (b) FESOL in 0.5 M HCl acid.

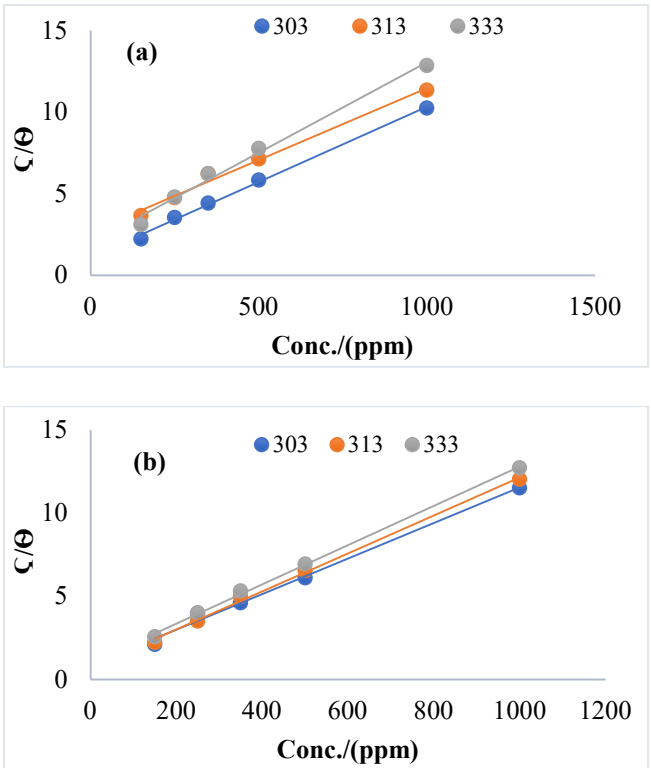

Fig. 7. Langmuir isotherm graphs for inhibition of 817M40T-Mild Steel without and with (a) AESOL and (b) FESOL in 0.5 M HCl acid.

Table 7. Langmuir Adsorption Values for Inhibition of 817M40T-Mild Steel without and with AESOL and FESOL in 0.5 M HCl Acid

	AESOL				FESOL			
Temp. (K)	k ($g\ l^{-1}$)	ΔG^*_{ads} ($kJ\ mol^{-1}$)	R^2	Slope	k ($g\ l^{-1}$)	ΔG^*_{ads} ($kJ\ mol^{-1}$)	R^2	Slope
303	0.91	-9.88	0.9919	0.009	1.19	-10.56	0.9937	0.011
313	0.51	-7.93	0.9902	0.011	1.39	-11.31	0.9975	0.012
333	0.38	-13.40	0.9893	0.009	0.99	-11.09	0.9985	0.011

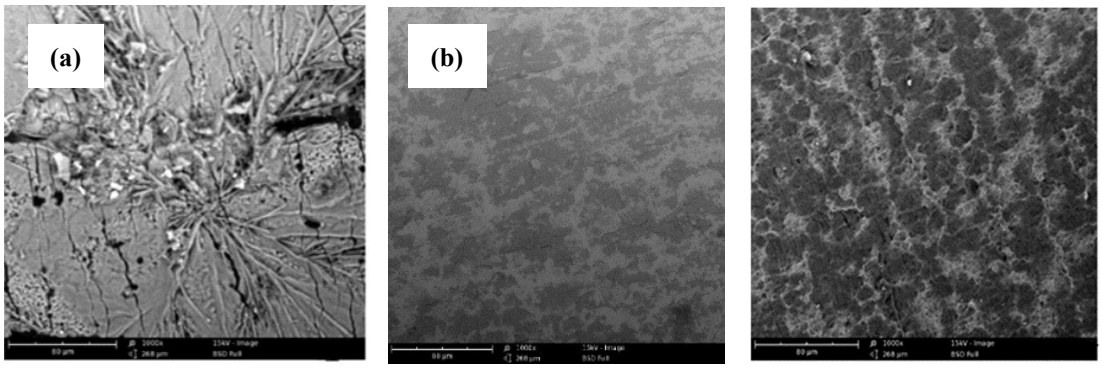

Fig. 8. Micrographs obtained for corrosion inhibition of mild steel in (a) 0.5 $M\ HCl$ (b) 1000 ppm solution of alkaloid extracts and (c) 1000 ppm solution of flavonoid extracts.

Scanning Electron Microscope Analysis

The nature of adsorption of the alkaloid and flavonoid extracts as inhibitions on 817M40T-Mild Steel was studied using scanning electron microscopy (SEM) [33-34]. This was possible through the study of the topography, morphology, and compositional information. Figure 8 shows the micrographs obtained for (a) metal in 0.5 $M\ HCl$ (b) in 1000 ppm solution of alkaloid extracts and (c) in 1000 ppm solution of flavonoid extracts. Analysis of the micrograph in Fig. 8a showed a very rough surface area which depicts the aggressive attack of the HClsolution on the metal due to the absence of the inhibitor [34]. However, the presence of the inhibitor at 1000 ppm concentration witnessed an appreciable decrease in metal surface roughness and complete smoothness. This could be arising from the large surface coverage area of the inhibitor on the metal surface, hence protecting anodic corrosive active sites from corrosion activation [30,39]. These micrographs show that both inhibitors are good inhibitors for the control of 817M40T-Mild Steel corrosion in HCl solution environment.

CONCLUSIONS

1. The corrosion rate effect of the inhibitors was seen to be in decrease from 1.6-0.01 and 1.6-0.1 while the inhibition efficiency values were in increase from 79.7%-99.3% and 75.1%-93.8% for alkaloid and flavonoid fractions respectively at 150-1000 ppm which defined the inhibitors a good inhibitors.
2. The inhibitors shifted the corrosion potential (E_{corr}) slightly to a more positive direction and also shows changes in both the cathodic and anodic polarization branches indicating a mixed-type inhibitor.
3. All results obtained from experimental work were in good agreement pointing to the efficacy of the inhibitors through the adsorption mechanism.
4. The inhibitors showed spontaneity and stability even at higher temperatures as thermodynamic values obtained were

at the threshold.

5. Result from the study of the topography, morphology, and compositional information showed a good inhibition of 817M40T-Mild Steel corrosion in 0.5 M HCl solution environment.

REFERENCES

[1] Bhuvaneswari, M.; Santhakumari, R.; Usha, C., Synthesis, growth, structural, Spectroscopic, optical, Thermal, DFT, HOMO-LUMO, MEP, NBO analysis, and Thermodynamic properties of vanillin isonicotinic hydrazide single crystal. *J. Mol. Struct*. **2021**, *4,* 130856. http://doi.org./10.1016/j.molstruc.2021.130856.

[2] Ahmed, A. F.; Hossam, E. A.; Emad, A. B.; Eslam, A. M.; Asmaa, I. A.; El-Etre, A. Y., The inhibition performance of morpholinium derivatives on corrosion behavior of carbon steel in the acidized formation water: Theoretical, experimental and biocidal evaluations. *J. Mol. Liqs*. **2021**, *341,* 117348 https://doi.org/10.1016/j.molliq.2021.117348.

[3] Dimakis, N.; Salas, I.; Gonzalez, L., Li and Na adsorption on graphene and graphene oxide examined by density functional theory, quantum theory of atoms in molecules, and electron localization function. *Molecules* **2019**, *24*, 754. http://doi.org./10.3390/molecules24040754.

[4] Joycee, S. C.; Raja, A. S.; Amalraj, A. S.; Rajendran, S., Corrosion mitigation by an eco-friendly inhibitor: Beta vulgaris (beeroot) extract on mild steel in simulated oil well water medium. *Int. J. Corros. Scale Inhib.* **2022**, *11*, 82-101. http://doi.org./10.17675/2305-6894-2022-11-1-4.

[5] Erteeb, M. A.; Ali-Shattle, E. E.; Khalil, S. M., Computationl studies (DFT) and PM3 theories on thiophene oligomers as corrosion inhibitors for iron. *Americ. J. Chem*. **2021**, *11,* 1-7. http://doi.org./10.5923/j.chemistry.20211101.01.

[6] Fajobi, M. A.; Fayomi, O. S. I.; Akande, I. G., Inhibitive Performance of Ibuprofen Drug on Mild Steel in 0.5 M of H_2SO_4 Acid. *J. Bio-Tribo. Corr*. **2019**, *5,* 1-5. http://doi.org./10.1007/s40735-019-0271-3.

[7] Fouda, A. E. S.; El-Askalany, A. H.; Molouk, A. F. S., Experimental and computational chemical studies on the corrosion inhibitive properties of carbonitrile compounds for carbon steel in aqueous solution. *Sci. Rep.* **2021**, *11*, 67-79. http://doi.org./10.1038/s41598-021-00701-z.

[8] Hashem, H. E.; Farag, A. A.; Eslam, A. M.; Eman, M. A., Experimental and theoretical assessment of benzopyran compounds as inhibitors to steel corrosion in aggressive acid solution. *J. Mol. Struct.* **2021**, *1249,* 131641. https://doi.org/10.1016/j.molstruc.2021.131641.

[9] Joshi, B. D.; Thakur, G.; Chaudhary, M. K., Molecular structure, homo-lumo and vibrational analysis of ergoline by density functional theory. *Sci. World.* **2021**, *14,* 21-30. http://doi.org./10.3126/sw.v14i14.34978.

[10] Ugi, B. U.; Obeten, M. E.; Ikeuba, A. I., Inhibition Efficiency of Eco-friendly Green Inhibitors (Ocimumtenuiflorumphyto - compounds) on Corrosion of High Carbon Steel in HCl Environment using Thermometric and Electrochemical Methods. *J. Adv. Electrochem.* **2018**, *4,* 158-161. https://doi.org/10.30799/jaec.052.18040102.

[11] Parajuli, D.; Sharma, S.; Oli, H. B.; Bohara, D. S.; Bhattarai, D. P.; Tiwari, A. P.; Yadav, A. P., Comparative study of corrosion in hibition efficacy of alkaloid extracts of Artemesia vulgaris and Solanum tuberosum in mild steel samples in 1 M sulphuric acid. *Electrochem*. **2022**, *3*, 416-433. http://doi.org./10.3390/electrochem3030029.

[12] Majda, M. T.; Ramezanzadeh, M.; Ramezanzadeh, B., Production of an environmentally stable anti-corrosion film based on Esfand seed extract molecules- metal cations: Integrated experimental and computer modeling approaches. *J. Hazard. Mater*. **2020**, *382,* 1-16. http://doi.org./10.1016/j.hazmat.20192019.121029

[13] Onyeachu, I. B.; Abdel-Azeim, S.; Chauhan, D. S., Electrochemical and Computational insights on the application of expired Metformin drug as a novel inhibitor for the sweet corrosion of C1018 steel. *ACS Omega.* **2021**, *6,* 65-76. http://doi.org./10.1021/acsomega.0c03364.

[14] Padash, R.; Sajadi, G. S.; Jafari, A. H., Corrosion control of aluminum in the solutions of NaCl, HCl and NaOH using 2,6-dimethylpyridine inhibitor:

Experimental and DFT insights. *Mater. Chem. Phys.* **2020**, *244,* 122681. http://doi.org./10.1016/j.matchemphys.2020.122681.

[15] Rbaa, M.; Ouakki, M.; Galai, M., Simple preparation and characterization of novel 8-hydroxyquinoline derivatives as effective acid corrosion inhibitor for mild steel: Experimental and theoretical studies. *Coll. Surf. A: Physicochem. Eng. Aspects*. **2020**, *602,* 125094. http://doi.org./10.1016/j.colsurfa.2020.125094.

[16] Bilgic, S., Plant extracts as corrosion inhibitors of mils ateel in H_2SO_4 and H_3PO_4 media-Review II. *Int. J. Corros. Scale Inhib.* **2022**, *11*, 1-42. http://doi.org./10.17675/2305-6894-2022-11-1-41.

[17] Sharma, S.; Ganjoo, R.; Saha, S. K., Experimental and theoretical analysis of baclofen as a potential corrosion inhibitor for mild steel surface in HCl medium. *J. Adhs. Sci. Tech*. **2021**, *1,*121. https://doi.org/10.1080/01694243.2021.200230.

[18] Su, P.; Li, L.; Li, W., Expired drug theophylline as potential corrosion inhibitor for 7075 aluminum alloy in 1 M NaOH solution. *Int. J. Electrochem. Sci.* **2020**, *15,* 1412-1425. http://doi.org./10.20964/2020.02.25.

[19] Tsygankova, L. E.; Uryadnikov, A. A.; Abramov, A. E.; Semenyuk, T. V., Inhibiting formulations against hydrogen sulfide corrosion of carbon steel. *Int. J. Corros. Scale Inhib.* **2022**, *11*, 102-110. http://doi.org./10.17675/2305-6894-2021-11-1-45.

[20] Geerlings, P.; Chamorro, E.; Chattaraj, P. K., Conceptual density functional theory: status, prospects, issues. *Theor. Chem. Account.* **2020**, *139,* 36 http://doi.org./10.1007/s00214-020-2546-7.

[21] Hsissou, R.; About, S.; Seghiri, R., Evaluation of corrosion inhibition performance of phosphorus polymer for carbon steel in [1 M] HCl: Computational studies (DFT, MC and MD simulations). *J. Mater. Resear. Tech.* **2020**, *9,* 2691-2703. http://doi.org./10.1016/j.jmrt.2020.01.002.

[22] Jiajun, F. U.; Su-ning, L.; Wang, Y., Computational and electrochemical studies of some amino acid compounds as corrosion inhibitors for mild steel in hydrochloric acid solution. *J. Mater. Sci.* **2020,** *45*, 6255-6265. http://doi.org./10.1007/s10853-010-4720-0.

[23] Ebenso, E. E.; Verma, C.; Olasunkanmi, L. O., Molecular modelling of compounds used for corrosion inhibition studies: a review. *Phys. Chem. Chem. Phys*. **2021**, *23,* 19987-20027. http://doi.org./10.1039/D1CP00244A.

[24] Agwamba, E. C.; Udoikono, A. D.; Hitler, L., Synthesis, characterization, DFT studies, and molecular modeling of azo dye derivatives as potential candidate for trypanosomiasis treatment. *Chem. Phys. Imp.* **2022**, *4*, 100076. http://doi.org./10.1016/chphi.2022.100076

[25] El-Monem, M. A.; Shaban, M. M.; Khalil, M. M. H., Synthesis, Characterization and computational chemical study of Aliphatic Tricationic surfactants for metallic equipment in oil fields. *ACS Omega.* **2020**, *5*, 26626-26639 http://doi.org./10.1021/acsomega.0c03432.

[26] Erazua, E. A.; Adeleke, B. B., A computational study of quinolone derivatives as corrosion inhibitors for mild steel. *J. Appl. Sci. Environ. Manage*. **2019**, *23,* 1819-1824. http://doi.org./10.4314/jasem.v23i10.8.

[27] Ugi, B. U.; Obeten, M.; Bassey, V.; BoEkom, E. J.; Omaliko E. C.; Ugi, F. B.; Uwah, I. E., Quantum and Electrochemical Studies of Corrosion Inhibition Impact on Industrial Structural Steel (E410) by Expired Amiloride Drug in 0.5 M Solutions of HCl, H_2SO_4 and $NaHCO_3$. *Mor. J. Chem.* **2021**, *9,* 677-696. https://doi.org/10.48317/IMIST.PRSM/morjchem-v9i3.22346.

[28] Bashir, S.; Sharma, V.; Kumar, S., Inhibition performances of Nicotinamide against aluminum corrosion in an acidic medium. *Port Electrochim. Acta*. **2020**, *38*, 107-123. http://doi.org./10.4152/pea.202002107.

[29] Kurls, E. A.; Ahmed, A. F.; Eslam, A. M.; Eman, M. A.; Galal, H. S., Corrosion inhibition performance and computational studies of pyridine and pyran derivatives for API X-65 steel in 6 M H_2SO_4. *J. Ind. Engr. Chem.* **2021**, *97,* 523-538, https://doi.org/10.1016/j.jiec.2021.03.016.

[30] Bharatiya, U.; Gal, P.; Agrawal, A., Effect of corrosion on crude oil and natural gas pipeline with emphasis on prevention by ecofriendly corrosion inhibitors: a comprehensive review. *J. Bio-Tribo. Corr*. **2019**, *5,* 35. http://doi.org./10.1007/s40735-019-0225-9.

[31] Tan, J.; Guo, L.; Wu, D., Electrochemical and computational studies on the corrosion inhibition of

mild steel by 1-hexadecyl-3-methylimidazolium Bromide in HCl medium. *Int. J. Electrochem. Sci.* **2020**, *15,* 1893-1903. http://doi.org./10.20964/2020.03.36.

[32] Kadhim, A.; Betti, N.; Al-Adili, A.; Shaker, L. M.; Al-Amiery, A. A., Limits and developments in organic inhibitors for corrosion of mild steel: a critical review (Part two: 4-aminoantipyrine). *Int. J. Corros. Scale Inhib.* **2022**, *11*, 46-63. http://doi.org./10.17675/2305-6894-2022-11-1-2.

[33] Thanh, L. T.; Vu, N. S. H.; Binh, P. M. Q., Combined experimental and computation studies on corrosion inhibition of Houttuynia cordata leaf extract for steel in HCl medium. *J. Mol. Liq*. **2020**, *315,* 113787. http://doi.org./10.1016/j.molliq.2020.113787.

[34] Ugi, B. U.; Obeten, M. E.; Bassey, V. M., Adsorption and inhibition analysis of aconitine and tubocurarine alkaloids as eco-friendly inhibitors of pitting corrosion in ASTM-A47 low carbon steel in HCl acid environment. *Indones. J. Chem.* **2022**, *22,* 1-16. http://doi.org./10.22146/ijc.56745.

[35] Xi, J.; Liu, C.; Morgan, D., An Unexpected Role of H During SiC Corrosion in Water. *J. Phys. Chem. C*. **2020**, *124,* 9394-9400. http://doi.org./10.1021/acs.jpcc.0c02027.

[36] Zaher, A.; Chaouiki, A.; Salghi, R., Inhibition of mild steel corrosion in 1M hydrochloric medium by the methanolic extract of *Ammi visnaga* l. Lam seeds. *Hindawi Int. J. Corr.* **2020**, *1,* 1-10. http://doi.org./10.1155/2020/9764206.

[37] Gadow, H. S.; Fakeeh, M., Green inhibition of carbon steel corrosion in 1 M hydrochloric acid: Eruca Sativa seed extract (experimental and theoretical studies). *RSC Adv*. **2022**, *12*, 8953-8986. http://doi.org./10.1039/D2RA01296K.

[38] Abdallah, M.; Gad, E. A. M.; Sobhi, M., Performance of tramadol drug as a safe inhibitor for aluminum corrosion in 1.0 M HCl solution and understanding mechanism of inhibition using DFT. *Egypt. J. Petrol.* **2019**, *28*, 173-181. http://doi.org./10.1016/j.ejpe.2019.02.003.

[39] Ammouchi, N.; Allal, H.; Belhocine, Y., DFT computations and molecular dynamics investigations on conformers of some pyrazinamide derivatives as corrosion inhibitors for aluminum. *J. Mol. Liq.* **2020**, *300*, 112309. http://doi.org./10.1016/j.molliq.2019.112309.

[40] Yoshiki, K.; Ahmed, A. F.; Etsushi, T.; Yoshitaka, A.; Hiroki, H., formation of porous anodic films on carbon steels and their application to corrosion protection composite coatings formed with Polypyrrole. *J. Electrochem. Soc.* **2016***, 163,* C386-C393. DOI: 10.1149/2.1451607jes.